

On the origin of the streak spacing in turbulent shear flows

By Fabian Waleffe

It is shown that the ideas of *selective amplification* and *direct resonance*, based on linear theory, can not provide an explanation for the well-defined streak spacing of about 100 wall units (referred to as 100^+ hereafter) in wall-bounded turbulent shear flows. In addition, for the direct resonance theory, the streaks are created by the non-linear self-interaction of the vertical velocity rather than of the *directly forced* vertical vorticity. In view of the failure of these approaches, it is then proposed that the selection mechanism must be inherently non-linear and correspond to a *self-sustaining* mechanism. The 100^+ value should thus be considered as a critical Reynolds number for that mechanism. Indeed, in the case of Poiseuille flow, this 100^+ criterion for transition to turbulence corresponds to the usually quoted value of 1000 based on the half-width and the centerline velocity. In Couette flow, it corresponds to a critical Reynolds number of about 400 based on the half width and half velocity difference.

1. Motivation and objectives

An intriguing feature of wall-bounded turbulent shear flows is the existence of bands of low- and high-speed fluid, elongated in the streamwise direction and with a very consistent spanwise spacing of about one hundred wall units, i.e. $100\nu/u_*$ where $u_* = (\nu dU/dy)^{1/2}$ is the friction velocity. In addition, those streaks appear to initiate a localized instability referred to as a "burst". That localized instability would be the mechanism by which momentum is exchanged between the wall and the outer fluid, thus sustaining the turbulent flow (Kline *et al.* 1967, Kim *et al.* 1971).

The goal of this project, performed in collaboration with John Kim, is to try to understand the mechanisms which lead to the creation and destruction of the streaks. We believe that those mechanisms are the key to understanding why and how a flow ceases to be laminar and maintains a turbulent state. Our approach was to first review and test some ideas which had been proposed in the literature for the origin of the streaks. If these theories were successful, our objective was then to extend them so as to explain the bursting and regeneration processes.

2. Work accomplished

2.1. RDT and selective amplification

A number of papers (e.g. Lee *et al.* 1990) show that the mechanism for streak generation is linear. The argument is that in the near wall-region the time scale for the mean $(d\bar{u}/dy)^{-1}$ is much shorter than the time scale for the non-linear effects,

measured by q^2/ϵ where q is a turbulent velocity scale and ϵ is the dissipation rate. The evolution is then dictated by linear equations, and streaks are created from the redistribution of the downstream momentum by vertical and spanwise motions. The mechanism is a simple advection and is most efficient when the fluctuating fields are elongated downstream. The question here is to determine whether the linear mechanism favors spanwise scales of about 100^+ . The mathematical description of the mechanism is briefly stated in the next few paragraphs.

The governing equations for the fluctuating field, obtained by eliminating pressure and the continuity constraint, are:

$$\left(\frac{\partial}{\partial t} + \bar{u} \frac{\partial}{\partial x} - \frac{1}{R} \nabla^2\right) \nabla^2 v - \frac{d^2 \bar{u}}{dy^2} \frac{\partial}{\partial x} v = NL_v \quad (1)$$

$$\left(\frac{\partial}{\partial t} + \bar{u} \frac{\partial}{\partial x} - \frac{1}{R} \nabla^2\right) \eta + \frac{d\bar{u}}{dy} \frac{\partial}{\partial x} v = NL_\eta \quad (2)$$

where v and η denote respectively the y -component of velocity and vorticity, and \bar{u} is the mean velocity. The right-hand sides, NL_v , NL_η , represent non-linear terms. Flows in a channel will be considered in this paper (plane Poiseuille or plane Couette flow) with the boundary conditions $v = \partial v / \partial y = \eta = 0$ at the walls, located at $y = \pm 1$.

In the linear case, the equation for v is homogeneous and admits eigensolutions of the form:

$$v = \hat{v}(y) e^{i(\alpha x + \beta z - \omega t)} \quad (3)$$

where $\hat{v}(y)$ satisfies the *Orr-Sommerfeld* equation. In general, for a turbulent mean profile, all of these eigensolutions are decaying. The η -equation, on the other hand, is non-homogeneous for v fluctuations with a spanwise variation. When forced by an eigenmode of the v equation, the linear response of the vertical vorticity has the form:

$$\eta = \eta(y, t) e^{i(\alpha x + \beta z)} \quad (4)$$

with $\eta(y, t)$ given by:

$$\eta(y, t) = \beta \sum_n \lambda_n \frac{e^{-i\omega t} - e^{-i\mu_n t}}{\omega - \mu_n} \eta_n(y) \quad (5)$$

Where

$$\lambda_n = \frac{\int \bar{u}' \hat{v} \eta_n dy}{\int \eta_n \eta_n dy} \quad (6)$$

and $\eta_n(y)$, μ_n represent the eigenmodes and eigenvalues of the homogeneous η -equation. Note that the vertical vorticity response corresponds to streaks, as opposed to vortices.

When the OS eigenvalue ω is close to the Squire eigenvalue μ_n , the n -th coefficient will behave as $t \exp(-i\mu_n t)$. This corresponds to an algebraic growth followed by exponential decay as μ_n corresponds to a viscously decaying mode. For a significant

algebraic growth to occur, the real parts of ω and μ must be sufficiently close otherwise the modes will decorrelate, and the viscous damping must be small. Thus one expects and verifies numerically that the largest responses occur for downstream modes ($\alpha = 0$) for which the real parts of the eigenvalues vanish (downstream modes are not advected) and the decay rate is inversely proportional to the Reynolds number. In fact the, eigenvalue problems can be solved analytically in that case, and one finds (with $n > 0$)

• even modes:

$$\begin{aligned} \eta_{2n-1}(y) &= \cos(2n-1)\frac{\pi}{2}y & \mu_{2n-1} &= -\frac{\beta^2 + (2n-1)^2\pi^2/4}{R} \\ v_{2n-1}(y) &= (\cosh \beta \cos p_n y - \cos p_n \cosh \beta y) & \omega_{2n-1} &= -\frac{\beta^2 + p_n^2}{R} \end{aligned}$$

• odd modes:

$$\begin{aligned} \eta_{2n}(y) &= \sin n\pi y & \mu_{2n} &= -\frac{\beta^2 + n^2\pi^2}{R} \\ v_{2n}(y) &= (\sinh \beta \sin q_n y - \sin q_n \sinh \beta y) & \omega_{2n} &= -\frac{\beta^2 + q_n^2}{R} \end{aligned}$$

where p_n and q_n are the solutions of:

$$\begin{aligned} p_n \tan p_n &= -\beta \tanh \beta \\ \beta \tan q_n &= q_n \tanh \beta \end{aligned}$$

and obey the ordering:

$$(2n-1)\pi/2 < p_n < n\pi < q_n < (2n+1)\pi/2$$

In the inviscid case, the streaks appear to grow indefinitely with time. However, the *exact* equation for the downstream velocity u is:

$$\frac{\partial}{\partial t}u + v\frac{\partial}{\partial y}u + w\frac{\partial}{\partial z}u = -\frac{\partial}{\partial x}P$$

where $\partial P/\partial x$ is a constant. This equation is linear, as v and w decouple, and expresses an advection of the momentum by the cross-stream flow. The term $v\partial u/\partial y$ creates the linear growth described above, creating $\partial u/\partial z$ which then limits the process through the term $w\partial u/\partial z$ which is considered "non-linear" in the preceding analysis. If ϵ is a measure of the amplitude of the cross stream flow (v, w), the "non-linear" saturation of the algebraic growth occurs on a time scale $O(\epsilon^{-1})$, the time scale for advection by the cross flow. It is faster than the usual ϵ^{-2} , characteristic of non-linear interactions.

The possibility of a scale selection by the linear mechanism was investigated numerically by introducing a downstream OS mode, normalized so that the maximum

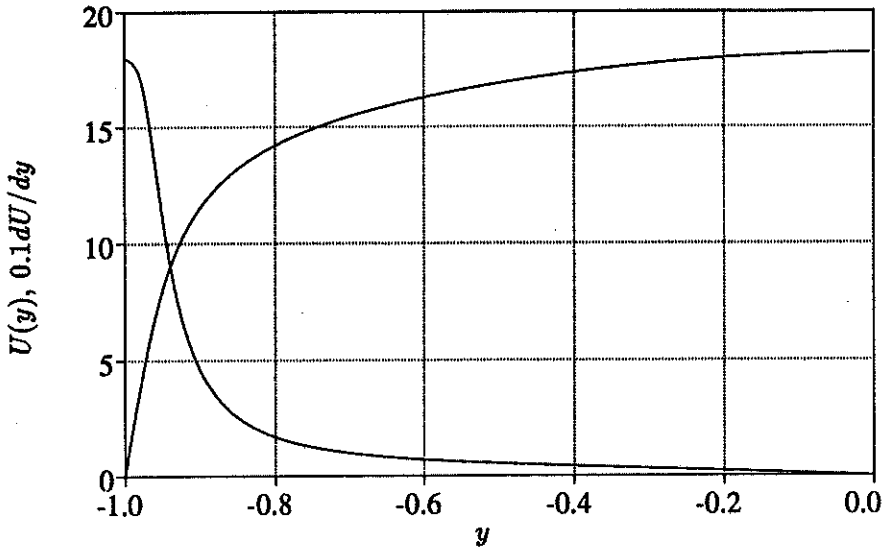


FIGURE 1. Mean profile and mean shear.

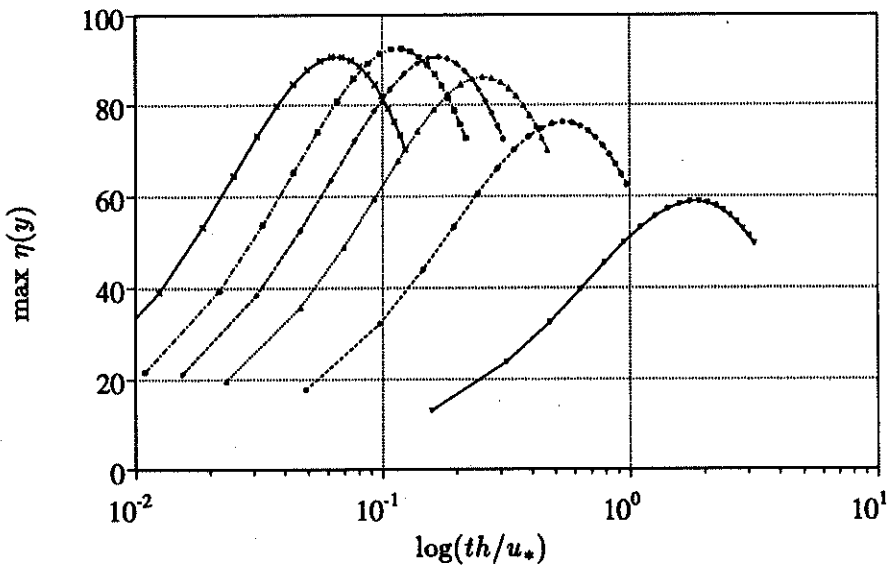


FIGURE 2. Maximum pointwise vertical vorticity response to a single downstream even OS mode. ∇ : $\lambda_z^+ = 188$; \bullet : $\lambda_z^+ = 94$; \triangle : $\lambda_z^+ = 63$; \diamond : $\lambda_z^+ = 47$; \square : $\lambda_z^+ = 38$; \times : $\lambda_z^+ = 27$.

vertical velocity is unity, onto a turbulent mean profile with $R_\tau = 180$. The mean velocity profile was chosen as a Reynolds-Tiederman profile, defined by :

$$\frac{d\bar{u}}{dy} = -\frac{Ry}{(1 + \nu_t)}$$

$$\nu_t = \frac{1}{2} \left\{ 1 + \left[\frac{1}{3} KR(1 - y^2)(1 + 2y^2)(1 - \exp((1 + y)R/A)) \right]^2 \right\}^{1/2} - \frac{1}{2}$$

where K and A were chosen respectively as 0.525 and 37. The mean profile and mean shear are shown in fig. 1.

The forced responses of the vertical vorticity are shown in fig. 2. It can be seen that there is a peak around $\lambda_z^+ = 35$, but it is too weak to represent a significant selection. The streamwise fluctuating velocity responses would be obtained by multiplying the vorticity by the wavelength, and the largest response would correspond to the largest wavelength. This does not match the experimental observations which show a scale selection both in the velocity and vorticity spectra. In any case, the "peak" does not correspond to the typical value for the streak spacing, which is between 80^+ and 100^+ . We must conclude that the linear mechanism does not provide a scale selection.

2.2. Direct resonance theory

In the direct resonance scenario, streaks originate from a three-step process (Benney and Gustavsson 1981, Jang *et al.* 1986). The first step is linear and consists of the resonant forcing of the vertical vorticity by the velocity, exactly as in the previous section, but focuses on oblique disturbances for which the non-linear effects can be less trivial. The second step is the non-linear interaction of the vorticity with its mirror image across a vertical downstream plane. This would create downstream vortices which, finally, give rise to the streaks. That sequence of interaction is illustrated by the following diagram.

$$\begin{aligned} \epsilon v(\alpha, \pm\beta) &\longrightarrow \epsilon t \eta(\alpha, \pm\beta) \\ \eta \eta^* &\longrightarrow v(0, 2\beta) \\ v(0, 2\beta) &\longrightarrow \eta(0, 2\beta) \end{aligned}$$

A non-linear theory was developed in (Benney and Gustavsson 1981) and applied to turbulent boundary layers in (Jang *et al.* 1986). Using a turbulent boundary layer profile, Jang *et al.* found that an OS eigenvalue coincides with a "Squire" eigenvalue (a *direct resonance*) for the horizontal wavenumbers: $\alpha^+ = 0.0093$ and $\beta^+ = 0.035$. The common eigenvalue is equal to $\omega^+ = 0.090 - i0.037$. They showed that the interaction of that mode with its spanwise reflexion induces streamwise vortices with a spanwise wavelength around $\pi/\beta^+ \simeq 90^+$.

One problem with the direct resonance concept is that it must assume not only that the eigenvalues of the two linear homogeneous operators are close, but also that the damping rates are small. Otherwise, as discussed above, the algebraic growth will be quickly shut off by the exponential viscous decay. Another problem

comes from multiple resonances or near-resonances. There is no *a priori* criterion for which one should prevail.

Here, the direct resonance route to streaks is followed in the case of a turbulent channel flow obtained numerically (Kim *et al.* 1987). The Reynolds number is about 180, based on the half-width and the friction velocity. A near direct resonance is found for :

$$\alpha^+ \simeq 0.005 \quad \beta^+ \simeq 0.039$$

the eigenvalues being:

$$\omega_{14}^+ = 0.07871485 - i 0.02168581$$

$$\mu_{15}^+ = 0.07871461 - i 0.02168558$$

These values are different but quite close to the values reported above for the turbulent boundary layer. The non-linear interaction of the pair of modes $(\alpha, \pm\beta)$ leads to streaks with a spanwise spacing of about 80^+ . The vertical vorticity responses are displayed in fig. 3. The initial conditions were such that the maximum v amplitude was 0.1 with no vertical vorticity. As indicated by the subscripts, this direct resonance occurs at the 14th OS mode and the 15th Squire mode, where the modes are ordered according to their decay rate. Although this looks encouraging, the picture is not as sharp when one analyzes other modes.

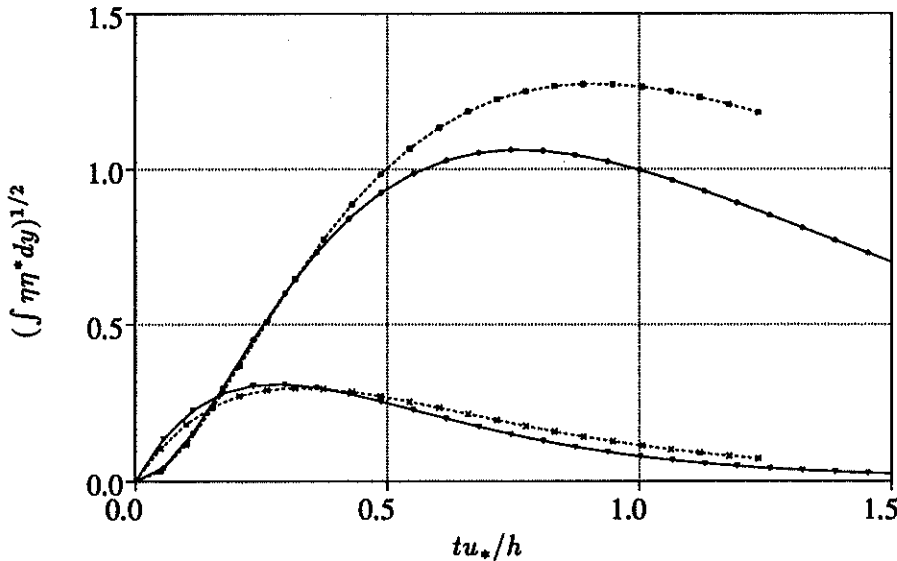


FIGURE 3. Linear (lower curves) and non-linear (upper curves) vertical vorticity response for direct resonance: ∇ : $(\alpha, \beta) = (0.9, 7.07)$ (forced by 14th OS mode); \bullet : $(0, 14.14)$; \times : $(0.8, 6)$ (forced by 13th OS mode); \square : $(0, 12)$.

For instance, the linear response obtained from the 13th OS mode for slightly different wavenumbers is very similar to the direct resonance mode, but the non-linear response is even larger (fig. 3.). Something seems very wrong once the

response to the 19th OS mode for $(\alpha, \beta) = (1.6, 12)$ has been computed (fig.4.). In that case, the linear response is almost four times larger than the direct resonance one, but the non-linear response is much smaller. One would expect that if the linear response is four times larger than for the direct resonance modes, the non-linear response should be sixteen times larger than in the direct resonance case.

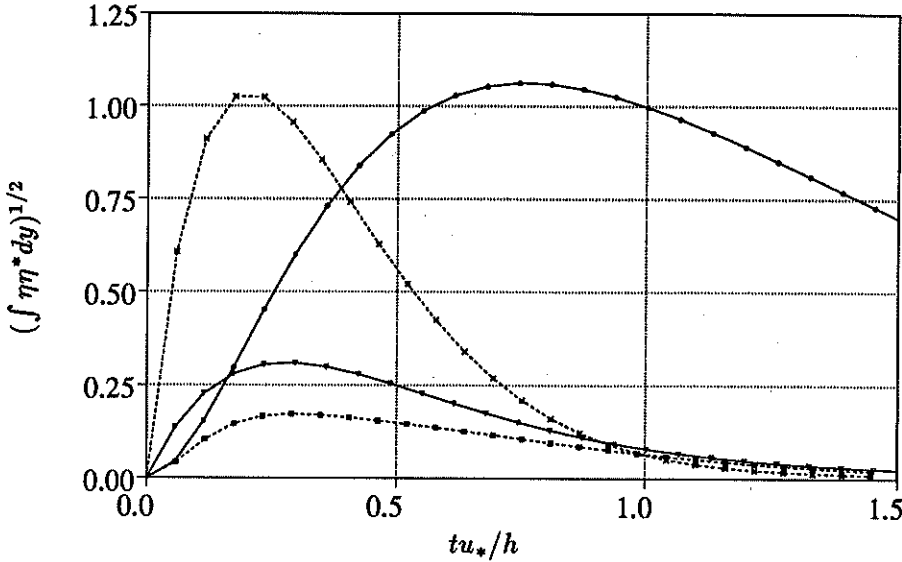


FIGURE 4. Linear and non-linear vertical vorticity response for direct resonance: ∇ : $(\alpha, \beta) = (0.9, 7.07)$ (forced by 14th OS mode); \bullet : $(0, 14.14)$; \times : $(1.6, 12)$ (forced by 19th OS mode); \square : $(0, 24)$.

To understand what went wrong, it is necessary to analyze the non-linear interactions. The computations and the theory are started with a pair of oblique rolls such as:

$$v = \cos \beta z (v_1(y, t)e^{i\alpha z} + v_1^*(y, t)e^{-i\alpha z})$$

The linear processes then introduce a pair of oblique streaks:

$$\eta = \sin \beta z (\eta_1(y, t)e^{i\alpha z} + \eta_1^*(y, t)e^{-i\alpha z})$$

The non-linear effect of primary interest is the generation of streamwise vortices $V(y, t) \cos 2\beta z$. The complete equation for $V(y, t)$ is obtained from (1) with the non-linear forcing provided by the pair of oblique rolls. After some manipulations (see e.g. Benney 1961, Lin and Benney 1962), one finds:

$$\left[\frac{\partial}{\partial t} - \frac{1}{R} \left(\frac{\partial^2}{\partial y^2} - 4\beta^2 \right) \right] \left(\frac{\partial^2}{\partial y^2} - 4\beta^2 \right) V =$$

$$\beta \left(\frac{\partial^2}{\partial y^2} + 4\beta^2 \right) (v_1 w_1^* + v_1^* w_1) + 4\beta^2 \frac{\partial}{\partial y} (v_1 v_1^* + w_1 w_1^*)$$

where w_1 is given in terms of v_1 and η_1 by

$$w_1 = k^{-2} \left(-\beta \frac{\partial v_1}{\partial y} + i\alpha \eta_1 \right)$$

with $k^2 = \alpha^2 + \beta^2$, so that the right-hand side can be rewritten as the sum of three forcing terms $F_{vv} + F_{v\eta} + F_{\eta\eta}$, where:

$$F_{vv} = 4 \frac{\alpha^2 \beta^2}{k^2} \frac{\partial}{\partial y} (v_1 v_1^*) + 4 \frac{\beta^4}{k^4} \frac{\partial}{\partial y} \left(\frac{\partial v_1}{\partial y} \frac{\partial v_1^*}{\partial y} \right) - \frac{\beta^2}{k^2} \frac{\partial^3}{\partial y^3} (v_1 v_1^*)$$

$$F_{v\eta} = \frac{i\alpha\beta}{k^2} \left[\left(\frac{\partial^2}{\partial y^2} + 4\beta^2 \right) (\eta_1 v_1^* - \eta_1^* v_1) + \frac{4\beta^2}{k^2} \frac{\partial}{\partial y} (\eta_1^* \frac{\partial}{\partial y} v_1 - \eta_1 \frac{\partial}{\partial y} v_1^*) \right]$$

$$F_{\eta\eta} = \frac{4\alpha^2 \beta^2}{k^4} \frac{\partial}{\partial y} (\eta_1 \eta_1^*)$$

In the direct resonance theory, the oblique streaks (η_1) are supposed to be much larger than the rolls so that only their non-linear interaction, i.e. the term $F_{\eta\eta}$, is considered. The three forcing terms are shown in fig. 5. for the direct resonance case at the time when $\eta(\alpha, \pm\beta)$ reaches its maximum amplitude (cf. fig.3).

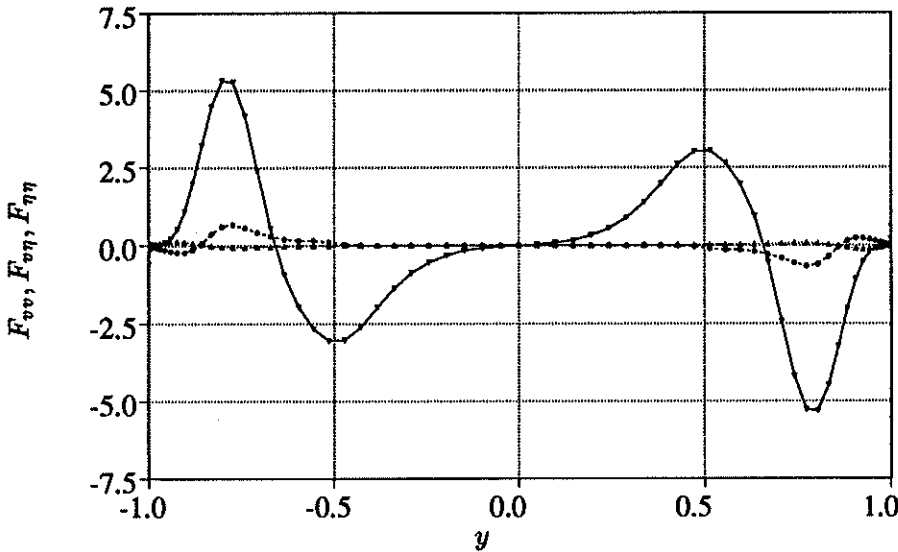


FIGURE 5. F_{vv} : ∇ , $F_{v\eta}$: \bullet and $F_{\eta\eta}$: \triangle at time when η is maximum. Computed for the direct resonance mode.

Figure 5 shows that the streamwise vorticity is the result of the non-linear interaction of the oblique rolls (v_1) and not of the "directly forced" oblique streaks (η_1). Thus the mechanism for the streamwise vorticity formation is the non-linear interaction of the vertical *velocity* of the oblique rolls, instead of the vertical *vorticity* as proposed in the direct resonance theory. We must conclude that the formation of streamwise vortices, and the streaks they induce, are not directly associated with "direct resonances".

2.3. Marginal flow

In view of the failure of the linear mechanism to provide a scale selection, we conclude that the selection must come from the original disturbance. In a turbulent flow the disturbance seems to arise from the breakdown of the streaks themselves (the bursting process). Thus the 100^+ selection must come from the complete *self-sustaining* mechanism. Our conjecture is that disturbances with a spacing smaller than about 100^+ can not be maintained. The 100^+ should then be considered as a *critical Reynolds number*. Experimental evidence for that proposal can be found in the work of Jimenez and Moin (1991). They show that for a channel flow at three different Reynolds numbers, $U_c h/\nu = 5000, 3000,$ and 2000 (U_c is the centerline velocity, h is the half-height), the flow returns to a laminar state when the spanwise width of the periodic box is reduced below about 100^+ .

We observe that for channel width of about 100^+ , the channel is very narrow. The characteristic length for the scaling of the disturbance should then be taken as the half width as opposed to the half height. In more general terms, the characteristic length should be taken as the smallest of half the channel height and width. Doing so, it turns out that "turbulence" disappears if $u_* \lambda_z/\nu < 100$ which corresponds to $U_c \lambda_z/(2\nu) < 1000$ ($\lambda_z/2$ is the half-width), irrespectively of the value of $U_c h/\nu$. But 1000 is the usually quoted value for the critical Reynolds number in channel flow. If one had reduced the height h as opposed to the width λ_z , "turbulence" would have also disappeared when $U_c h/\nu < 1000$ or $u_* h/\nu < 100$.

In order to capture the self-sustaining process in its simplest form, the next step is to reduce both dimensions ($2h$ and λ_z) to their minimum value so as to eliminate all unnecessary scales. One should be reminded at this point that the streaks are expected to be an essential element of the whole mechanism. The streaks are created from the redistribution of downstream momentum. From the distribution of the mean shear in a channel flow, the simplest self-sustaining non-laminar flow should then consists of a pair of opposite streaks in the spanwise direction and in the direction perpendicular to the walls as well, i.e one pair of streaks in either half of the channel. In Couette flow, where the mean shear has only one sign, the simplest solution should correspond to only one pair of streaks in the middle of the channel. Thus the simplest marginal channel flow should have dimensions $u_* 2h/\nu \simeq 100$ and $u_* \lambda_z/\nu \simeq 100$, while the simplest marginal Couette flow should have $u_* 2h/\nu \simeq 50$ and $u_* \lambda_z/\nu \simeq 100$.

A number of simulations of both flows support the above reasoning. "Turbulent" Couette flow could not be maintained at Reynolds numbers of 324 and below (based on the half height and half velocity difference) but was maintained for over 2000 convective time units ($2h/2U_w$) at a Reynolds number $U_w h/\nu = 400$. Thus the non-laminar flow was maintained for over five viscous units (h^2/ν), a time scale over which the slowest decaying scales would decay by a factor $\exp(-2.5\pi^2)$ if they were not sustained. The computed flows show considerable similarity with the near wall-region of higher Reynolds number flows. The main mechanism appears to be the breakdown of the streaks due to a spanwise inflectional instability. That instability seems to roll up, creating vortices inclined downstream, probably because of the

effect of the mean vertical shear. These vortices then proceed to recreate the streaks. However, this latter part of the complete process is still somewhat too disordered to firmly establish the mechanisms at play. It is hoped that imposing symmetries will further constrain the mechanism and clarify the nature of the fundamental self-sustaining flow.

REFERENCES

- BENNEY, D. J. 1961 A non-linear theory for oscillations in a parallel flow. *J. Fluid Mech.* **10**, 209-236.
- BENNEY, D. J. & GUSTAVSSON, L. H. 1981 A New Mechanism for Linear and Nonlinear Hydrodynamic Stability. *Studies in Appl. Math.* **64**, 185-209.
- JANG, P. S., BENNEY, D. J. & GRAN, R. L. 1986 On the origin of streamwise vortices in a turbulent boundary layer. *J. Fluid Mech.* **169**, 109-123.
- JIMENEZ, J. & MOIN, P. 1990 The minimal flow unit in near wall turbulence. *CTR Manuscript 105*. Center for Turbulence Research, Stanford University and NASA Ames Research Center. To appear in *J. Fluid Mech.*
- KIM, J., MOIN, P. & MOSER, R. D. 1987 Turbulence statistics in fully developed channel flow at low Reynolds number. *J. Fluid Mech.* **162**, 339-363.
- KIM, H. T., KLINE, S. J. & REYNOLDS, W. C. 1971 The production of turbulence near a smooth wall in a turbulent boundary layer. *J. Fluid Mech.* **50**, 133-160.
- KLINE, S. J., REYNOLDS, W. C., SCHRAUB, F. A. & RUNSTADLER, P. W. 1967 The structure of turbulent boundary layers. *J. Fluid Mech.* **30**, 741-773.
- LEE, M. J., KIM, J. & MOIN, P. 1990 Structure of turbulence at high shear rate. *J. Fluid Mech.* **216**, 561-583.
- LIN, C. C. & BENNEY, D. J. 1962 On the instability of shear flows. *Am. Math. Soc., Proc. Symp. Appl. Math.* **13**, 1.
- WALEFFE, F. 1989 Organized motions underlying turbulent shear flows. *CTR Annual Research Briefs.* **89**, 107-115.